Optical properties of itinerant UGa_3: Ellipsometric measurements and first-principles theory

J. Schoenes, U. Barkow, and M. Broschwitz
Institut für Halbleiterphysik und Optik, Technische Universität Braunschweig, Mendelssohnstrasse 3, D-38102 Braunschweig, Germany

P. M. Oppeneer
Institute of Solid State and Materials Research, P.O. Box 270016, D-01171 Dresden, Germany

D. Kaczorowski and A. Czopnik
Institute of Low Temperature and Structure Research, Polish Academy of Sciences, P.O. Box 1410, PL-50-950 Wrocław, Poland
(Received 17 August 1999)

The optical properties of the intermetallic compound UGa_3 have been determined by means of ellipsometric measurements. To cover the range from 0.7 to 9.5 eV a laboratory ellipsometer and a synchrotron ellipsometer have been used. The experimental results are compared to a computation of the optical properties from a first-principles band-structure calculation on the basis of local spin-density functional theory. The rather good agreement between the calculated and experimental spectra corroborates the itinerant character of the $5f$ electrons in UGa_3.

I. INTRODUCTION

The compound UGa_3 is a member of the large family of uranium binaries UX_3, which crystallize in the cubic structure of the $AuCu_3$ type. Depending on whether X is a p-band or d-band element various magnetic behaviors are observed, spanning from Pauli paramagnetism (USi_3, UGe_3), through spin-fluctuating heavy fermion (USn_3), to long-range local-moment magnetic ordering (UPb_3). The uranium gallide occupies a special position among the UX_3 phases (with X being an element from group IIIA of the Periodic Table), in between weakly temperature-dependent paramagnetic UAl_3 and antiferromagnetic UIn_3. The compound orders antiferromagnetically[1,2] at $T_N = 67$ K and exhibits metallic conductivity.[3,4] Comprehensive studies of the bulk magnetic, electrical transport, and thermal characteristics of poly- and single-crystalline UGa_3 (Refs. 5–7) have revealed that its magnetism has an itinerant-electron nature. This hypothesis has recently been corroborated by neutron diffraction measurements of the magnetic properties of a single crystal where a significant difference in the magnetic form factor determined above and below T_N has been evidenced.[8] Such a behavior is reconciled with the theory of itinerant antiferromagnetism.[8] The electronic structure of UGa_3 has been calculated by several authors on the basis of local spin density-functional theory.[9–12] It has been established that the $5f$ electrons form a narrow band near the Fermi level that is strongly hybridized with the broad conduction band of spd character. A characteristic feature of itinerant magnetism in UGa_3 is its unusual sensitivity to pressure and magnetic field, both factors causing a drastic reconstruction of the Fermi surface.[5–7,12]

Optical spectroscopy is a powerful and nondestructive technique to study the electronic structure of solids. Several actinide and rare-earth compounds and alloys have been studied in great detail and important conclusions about the energy, the width, and the degree of localization of f states could be drawn.[13] The most frequently used technique has been the measurement of the near-normal incidence reflectivity over a wide energy range and the subsequent Kramers-Kronig transformation of the spectra to compute the optical conductivity. While this technique gives excellent data if single crystals are available and can be cleaved, serious problems can arise if the surface has to be polished. The polishing process introduces scratches that scatter the light. Generally, the measured reflectivity deviates more from the true reflectivity the higher the photon energy.[13] Via the Kramers-Kronig integral, parts of these errors are spread over the full optical conductivity spectrum. The optical conductivity comes out too low, mainly at higher energies. Thermal annealing, chemical or electrochemical etching may help to heal or to remove the damaged surface. However, every new material will require a detailed study of the necessary parameters to prevent the formation of a nonstoichiometric surface by a preferred evaporation or solution of one of the constituents. To our knowledge, this procedure has not yet been applied successfully to actinides. An attempt for $MnPt_3$ gave poor results for thermal annealing as well as for chemical etching. In the latter case the magneto-optical Kerr rotation and ellipticity could at least be improved but the optical reflectivity decreased.[14]

An interesting alternative to the measurement of the reflectivity over a large spectral range constitutes ellipsometry. In this case, one is independent of an integral relation and the errors at high energies do not affect the data at lower energies. In addition, since one does not measure a reflected intensity, but the azimuth and the ratio of the small to the large axis of the polarization ellipse after reflection, isotropic scattering losses are expected to cancel each other. A quantitative description of the scattering due to polishing scratches on the surface is complex and outside the scope of this paper. There exist some models which can be useful in limiting cases. Specifically, if the diffracting object is large compared to the wavelength λ of the radiation, Kirchhoff's theory of diffraction is a valuable approach (see, for example, Ref. 15). This scalar theory gives a scattering which is independent of

the polarization, indicating that the reflected intensity is identical for parallel and perpendicular polarization and equal to

$$R = R_0 \exp\left[-\left(\frac{4\pi\sigma_{rms}}{\lambda} \right)^2 \right], \quad (1)$$

where R_0 is the reflectivity of the perfectly smooth sample and σ_{rms} is the root-mean-square value of $\zeta(x,y)$, expressing the roughness of an x-y surface. Besides neglecting the vector character of the electromagnetic field, Kirchhoff's theory does not take into account interactions between diffracting objects. Since our samples have obtained a final polishing with diamond paste with a grain size of 250-nm diameter the scattering structures are smaller than 250 nm and Kirchhoff's theory does not apply. A model which treats the scattering of light off particles that are smaller than the wavelength is Mie's theory.[16] In this theory the scattering of a planar wave off metallic spheres is treated in sperical coordinates. The solution leads to an expansion in series of electric and magnetic partial waves. The first electric partial wave corresponds to Rayleigh scattering and goes as $1/\omega^4$. Its consideration is sufficient if the diameter of the particle is smaller than approximately one-tenth of the wavelength of light inside the particle, i.e., $2r < \lambda/(10n)$, where n is the refractive index of the scattering particle. For larger particles more and more partial waves have to be taken into account and the frequency dependence of the scattering is reduced from the $1/\omega^4$ dependence. Interference effects can cause enhancements or reductions of the transmitted intensity.[17] Mie's theory also neglects interactions between the particles, and of course, a rough surface is not composed of sperical particles. Nevertheless, from the size of the scratches, which we estimate to be in the order of one-tenth of the polishing grain diameter, i.e., about 25 nm, we think that the theories of Mie or Rayleigh are better starting points to a qualitative discussion of scattering losses than Kirchhoff's theory. In any case both limits, Kirchhoff's and Rayleigh's theories, predict a scattering which increases with decreasing wavelength, in agreement with the experience of many materials for which the reflectivity has been measured on polished and cleaved crystals.[13] As long as the polarization dependence of scattering can be neglected, ellipsometry ought to give better data for the reflectivity and the other optical functions than near-normal incidence-reflectivity measurements on polished surfaces.

The drawback of ellipticity measurements is that they require polarizing devices and that the spot at the sample site is larger under oblique than under normal incidence. The latter can lead to a reduction of the intensity falling on the detector for the usual small size of ''exotic'' materials and the former fact limits even more the spectral range. To extend the spectral range beyond the range of 0.7 to 4 eV of our laboratory ellipsometer, we have used the synchrotron source in Berlin (BESSY I). Here we report for an actinide compound, ellipsometric measurements between 0.7 and 4 eV taken at Braunschweig with a xenon high-pressure lamp and between 3 and 9.5 eV taken at BESSY I with a 2m-Seya monochromator.[18]

The powerfulness of optical spectroscopy as a technique to investigate the electronic structure becomes even more impressive when measured optical spectra are combined with first-principles calculations. This is particularly relevant for the study of lanthanide and actinide compounds. For these *f*-electron compounds, the pertinent question that is to be addressed always is that of the degree of localization, i.e., whether the f's are localized or delocalized. In the case of transition metals, where the *d* electrons are delocalized, the general experience that was gained from optical property calculations is that normally first-principles band-structure theory, employing the local spin-density approximation[19,20] (LSDA) provides a very good explanation of the measured spectra. On the contrary, for *f*-electron materials where the f's are localized or have a tendency towards localization, the LSDA description can be quite poor. In that case alternative electronic structure approaches, like the LSDA+U method, or treating the f's as semicore electrons, have to be invoked to achieve a satisfactory explanation of the optical properties. A prominent example of that situation among the uranium compounds is that of the uranium monochalcogenides.[21–24] The important notion that has evolved from optical property calculations for *f*-electron materials is that the appropriate description of the f's will reproduce the measured optical spectrum.[25,26] Using this notion, it has been demonstrated in the last few years for several uranium compounds that these have delocalized $5f$ electrons.[26–28] In light of this notion, we investigate in the present work the nature of the $5f$'s in UGa_3 from the optical properties.

In the following we first outline in Sec. II the sample preparation and experimental optical setup, and the basics of the theory in Sec. III. Our results are presented and discussed in Sec. IV, and conclusions are formulated in Sec. V.

II. EXPERIMENT

Single crystals of UGa_3 were grown by the flux method. The starting constituents (8 at.% U+92 at.% Ga) were placed in an alumina crucible, vacuum sealed in a quartz tube and heated in a resistance furnace up to 1100 °C, held at this temperature for 48 h and eventually slowly cooled down to 450 °C at the rate of 8 deg/h. The excess of metallic Ga was removed by dissolving in Wood's alloy. The obtained single crystals had the form of cubes of a few mm on a side. X-ray diffraction measurements by the Laue technique showed the natural faces of the cubes to be typically (001) planes.

The single crystals of UGa_3 have been polished consecutively with corundum and diamond polishing pastes with grain sizes decreasing from 15 to 0.25 μm. The surfaces obtained are mirrorlike to the naked eye. However, under an optical microscope with high magnification one observes scratches, inhomogeneities, and dendrites. An attempt to improve the surface quality by removing electrochemically the uppermost layer failed. The surface appeared to be stable against chemical degradation including oxidation. The samples were mounted in the sample holders of the two spectrometers and the chamber was evacuated in the vacuum-UV spectrometer to a pressure of 10^{-8} Torr, while in the infrared and the visible spectral range the measurements were performed in air.

The laboratory spectrometer is a rotating analyzer ellipsometer (RAE). The polarizer and analyzer are Glan-Thompson prisms made from quartz. The analyzer is driven

by a synchronous motor with a frequency of 9 Hz. During one rotation of the analyzer 72 points on the ellipse are recorded, from which the azimuth θ_r and the ellipticity $\eta = a/b$ of the reflected light are derived using a Fourier analysis. Since the sample is mounted on a goniometer, the angle of incidence α of the light from the monochromator can be varied continuously from 60° to 85°. The present measurements have been performed with $\alpha = 75°$. The azimuth of the incoming light θ_i was chosen as 60° and the detector was a silicon-pin diode or a cooled Ge detector.

The BESSY ellipsometer also uses a rotating analyzer, with 50 measurements for 360° rotation of the analyzer. Since the polarization direction of the synchrotron radiation is fixed the polarization direction of the incoming light must be rotated out of the plane of incidence of the sample by tilting the whole spectrometer. This limits the azimuth of the incoming light to 20°. The angle of incidence is 67.5° and the light detector is a UV-sensitive silicon-pin diode.

III. THEORY

First-principles calculations of optical properties commonly apply the Kubo linear-response formalism, which relates the optical conductivity to the electronic structure of the solid. The linear-response expression for the diagonal component of the optical conductivity is, in a single-particle formulation, given by

$$\sigma(\omega) = \frac{-ie^2}{3m^2\hbar V_{uc}} \sum_{\boldsymbol{k}} \sum_{nn'} \frac{f(E_{n\boldsymbol{k}}) - f(E_{n'\boldsymbol{k}})}{\omega_{nn'}(\boldsymbol{k})} \times \frac{\Pi^2_{nn'}(\boldsymbol{k})}{-\omega + \omega_{nn'}(\boldsymbol{k}) + i\tau^{-1}}. \quad (2)$$

Here $E_{n\boldsymbol{k}}$ are the single-particle band energies, $f(E_{n\boldsymbol{k}})$ is the Fermi-Dirac distribution, V_{uc} the unit-cell volume, and $\hbar\omega_{nn'}(\boldsymbol{k}) \equiv E_{n\boldsymbol{k}} - E_{n'\boldsymbol{k}}$. A phenomenological lifetime parameter τ is included in the formalism in order to account approximately for the finite lifetime of the optically excited Bloch electron states. The dipole allowed optical transitions between the single-particle states $|n\boldsymbol{k}\rangle$ and $|n'\boldsymbol{k}\rangle$ are selected by the matrix elements of the relativistic momentum operator, $\boldsymbol{\Pi}_{nn'} = mc\langle n\boldsymbol{k}|\boldsymbol{\alpha}|n'\boldsymbol{k}\rangle$, where $\boldsymbol{\alpha}$ is the standard Dirac matrix. The present formulation is relativistic, because this is mandatory for actinide compounds in which the spin-orbit splitting of the $5f$ energy levels is of the order of 1 eV. In the limit of vanishing relativistic effects the canonical momentum is regained, $\boldsymbol{\Pi} \approx -i\hbar\boldsymbol{\nabla} + \mathcal{O}(1/c^2)$.[23] The single-particle wave functions $|n\boldsymbol{k}\rangle$ and energies $E_{n\boldsymbol{k}}$ that occur in Eq. (2) are calculated within the framework of the LSDA.[19,20]

Equation (2) contains both the interband (i.e., $n \neq n'$) and the intraband ($n = n'$) contribution to the optical conductivity. The latter contribution is, for zero temperature, due to electron states at the Fermi energy, and contributes therefore only at small photon energies. It adopts the form of a Drude-type conductivity, $\sigma^{intra} = \sigma_0/(1 + i\omega\tau_D)$. The intraband lifetime τ_D and the interband lifetime τ of the excited states (which can be different) are the only two unknown quantities in Eq. (2). However, approximate values are known both from experiments and from previous experience gained from *ab initio* calculations.[29] Thereby all is known that is required for the first-principles calculation of the optical conductivity. In the present work we employ a relativistic version of the augmented-spherical-wave (ASW) method[30] to evaluate the LSDA band energies and wave functions. For numerical details of the computation of Eq. (2) at zero temperature we refer to Ref. 29.

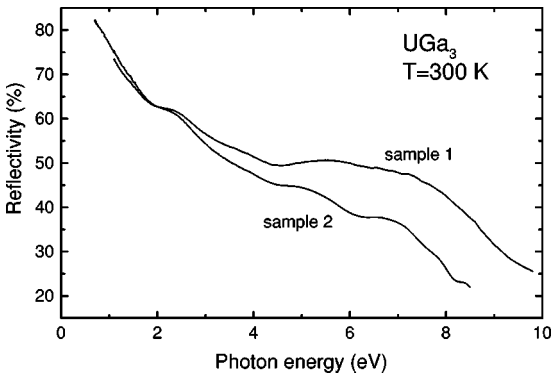

FIG. 1. The reflectivity of UGa_3 as calculated from ellipsometric measurements on two different samples at 300 K. The difference in the high-energy reflectivity is expected to result from the different surface quality.

IV. RESULTS AND DISCUSSION

A. Experimental determination of $\sigma(\omega)$

From the rotation of the azimuth $\theta = \theta_r - \theta_i$, where r and i stand for reflected and incident beam, respectively, and the ellipticity η one computes the complex reflection ratio for light polarized parallel and perpendicular to the plane of incidence:

$$\rho = \frac{r_p}{r_s} = \frac{(\cot\theta - i\eta)(\tan\theta_i + i\gamma_p)}{(1 + i\eta\cot\theta)(1 - i\gamma_p\tan\theta_i)}. \quad (3)$$

The coefficient γ_p takes into account the nonperfect polarization of the polarizer. The complex dielectric function $\varepsilon(\omega)$ follows as

$$\varepsilon = \left(\frac{1-\rho}{1+\rho}\right)^2 \tan^2\alpha \sin^2\alpha + \sin^2\alpha. \quad (4)$$

For metals it is preferable to plot the optical conductivity $\sigma(\omega) = \sigma_1(\omega) + i\sigma_2(\omega)$, given by

$$\sigma = i\frac{\omega}{4\pi}(\varepsilon - 1). \quad (5)$$

The multiplication of $\varepsilon(\omega)$ with ω reduces the strong frequency dependence of the free carriers and allows for a better comparison of experiment and theory for the interband transitions. Two measurements have been performed with both spectrometers for two different, polished surfaces. Figure 1 exhibits the reflectivity spectra $R(\omega)$ for the two surfaces as computed from the complex dielectric function. We see that for a different surface quality the difference of the reflectivities still increases with increasing photon energy, although to first order, scattering losses are expected to drop out of the reflectivity computed from ellipsometric measurements. This indicates either that the scattering is polarization

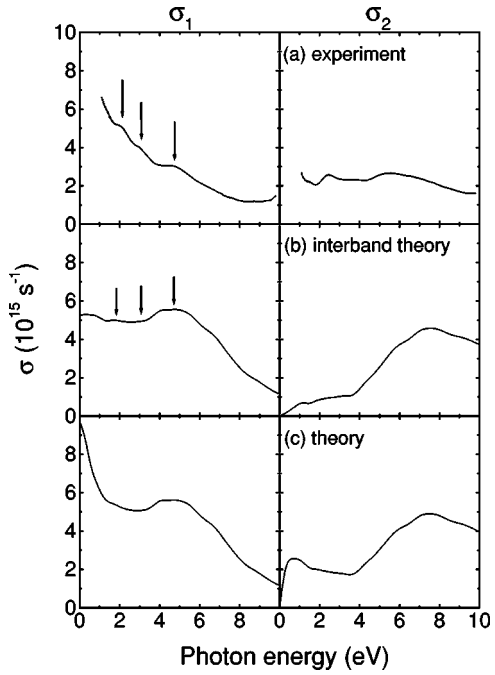

FIG. 2. Comparison of the experimental and calculated conductivity $\sigma(\omega)=\sigma_1(\omega)+i\sigma_2(\omega)$ of UGa_3. The experimental conductivity at 300 K is shown in the top panels (a). Note that $-\sigma_2(\omega)$ is depicted in the right-hand panels. The calculated interband conductivity is given in the middle panels (b), and the total theoretical (intraband plus interband) conductivity in the bottom panels (c).

dependent and thus affects the reflectivity ratio or that the polishing breaks local symmetries of the surrounding of the atoms which alters the electronic structure. Since both spectra show similar structures, we conclude that the observed structures are likely to be intrinsic to UGa_3 but we have to admit that a perfect surface would possibly have larger reflectivities and optical conductivities in the high energy range.

The obtained reflectivity (Fig. 1) and optical conductivity spectra, which are shown in Fig. 2 (top panels), are typical for metals. $R(\omega)$ and $\sigma_1(\omega)$ decrease from large values at low photon energies to small values at large photon energies. However, there is no clear plasma minimum. This is in contrast to the spectra found in the uranium monochalcogenides[13,31] and resembles more the case of uranium.[31,32] Thus on empirical grounds, UGa_3 appears to be a material with strongly hybridized conduction states. There is neither an indication of free electrons with small damping, nor a sharp peak which one might assign to a transition from narrow *f* states into a conduction band. This qualitative discussion gains support from the comparison with theory, which is addressed in the following.

B. Comparison experiment and theory

As we mentioned already in the Introduction, the LSDA band structure of paramagnetic UGa_3 was calculated recently by various methods, *viz.*, the nonrelativistic tight-binding method,[9] the full-potential linear-muffin-tin-orbital (LMTO) method,[10,11] and the relativistic ASW method.[12] The latter study also investigated the ground-state total energies of both (collinear) ferromagnetically and antiferromagnetically ordered UGa_3, which proved the ground state to be antiferromagnetically ordered. We have calculated the optical conductivity of UGa_3 in the paramagnetic and in the antiferromagnetic state. The obtained conductivity spectra are practically identical. In Fig. 2 the experimental $\sigma_1(\omega)$, $\sigma_2(\omega)$ are shown in the two top panels, in the two middle panels we show the calculated interband-only σ_1 and σ_2, and in the two bottom panels the total theoretical σ spectra, i.e., intra- and interband added. The obvious effect of the intraband Drude part is to increase σ_1 and σ_2 below 2 eV, in accordance with the experimental shape. We have depicted the small peaks visible in the measured σ_1 spectrum by arrows. These peaks, which are caused by strong interband optical transitions, are expected to be characteristic for the material. From the middle panels it can be seen that very similar weak peaks are present in the calculated interband-only σ_1 spectrum. The energy positions of the theory peaks are consistent with experiment, but the calculated ''hump'' at 5 eV is broader than the corresponding experimental peak. Also the theoretical σ_1 does not drop-off as much as the experimental σ_1 does. The interband-only σ_1 shows, furthermore, a shoulder just below 7 eV which very vaguely is present in experiment, too. The measured σ_2 spectrum is smaller than the theory result, especially above 5 eV. As σ_2 is related to σ_1 through a Kramers-Kronig transformation, this is again due to the stronger decrease of the measured σ_1. As we mentioned before, a perfect surface would lead to larger optical conductivities in the high-energy range.

With respect to our computation, we remark that a constant interband lifetime $\hbar\tau^{-1}=0.41$ eV has been applied. The intraband lifetime used is $\hbar\tau_D^{-1}=0.54$ eV and the calculated intraband Drude conductivity $\sigma_0=4.4\times10^{15}\,\mathrm{s}^{-1}$. In the calculations we included the Ga $4d$ states in the basis. These are unoccupied, yet play a role by providing allowed final states for optical transitions from the occupied Ga $4p$ states.

The small peaks in $\sigma_1(\omega)$ are the features typical of UGa_3. Which parts of the band structure are responsible for these? In the band structure there are too many hybridized bands to make an identification tractable. However, we may address the question from a consideration of the transition-matrix elements (ME). In our calculation the unit-cell volume is divided into atomic spheres around the nuclei and a tiny interstitial volume. Therefore the integral over the whole unit cell for the dipole matrix elements can be written as a sum over an integral over the spheres about U and about the galliums and over the interstitial (see Ref. 29). In the calculation we can ''by hand'' switch off the contribution to $\mathbf{\Pi}_{nn'}$ on either the U or on the Ga spheres. The $\mathbf{\Pi}$'s are thus separated in U and Ga contributions, but the band energies used for computing Eq. (2) are the hybridized $E_{n\boldsymbol{k}}$ of UGa_3. In Fig. 3 we show the result of this procedure on the calculated interband conductivity. The top panels of Fig. 3 gives the experimental $\sigma_1(\omega)$, $\sigma_2(\omega)$ for sake of comparison. The middle panels show σ_1, σ_2 computed with the U ME's switched off and the bottom panels with the Ga ME's switched off. The correspondence between the experimental conductivities and the ones calculated with transitions on the galliums only is immediately seen. The three small peaks in the measured σ_1 are present in the calculation with the ME's

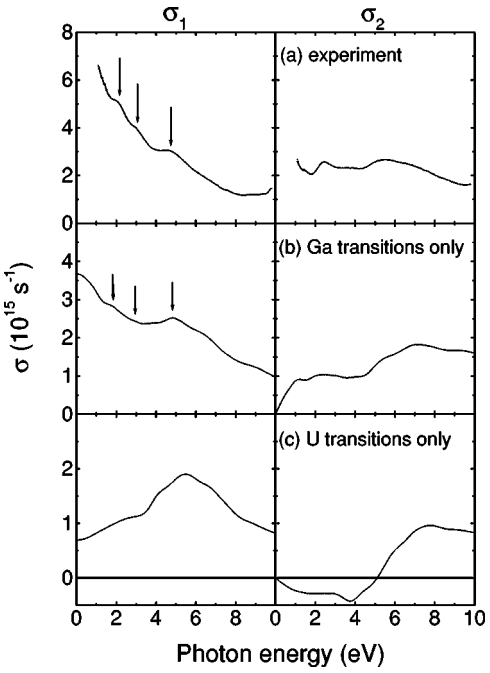

FIG. 3. Decomposition of the calculated interband optical conductivity in contributions on the Ga atoms and on the U atom. The middle panels (b) show the resulting σ_1, σ_2, when the optical matrix elements on U are switched off, i.e., only transitions on the Ga are taken into account. The bottom panels (c) show the resulting spectra when only the transitions on U are accounted for. The top panels (a) depict the experimental σ_1, σ_2 for comparison.

on U switched off (see the arrows in Fig. 3), but not when the Ga ME's are switched off. The characteristic peaks are thus dominantly due to optical interband transitions on the galliums. The broad hump at 4–6 eV in the interband-only σ_1 is mainly due to transitions on U. This hump is only weakly present in the measured σ_1. A tentative explanation for chemically or electrochemically treated surfaces could be that the surface becomes Ga rich. We emphasize, however, that the samples used were not treated chemically or electrochemically. In addition, we note that the fact that the band energies of UGa_3—and not those of Ga—are used in the computation of Eq. (2) implies that the hybridized UGa_3 bands in combination with the ME's are responsible for the three peaks.

V. CONCLUSIONS

We have employed the optical properties of UGa_3 to investigate the nature of the $5f$ electrons. The complex optical conductivity has been determined by means of ellipsometric measurements from 0.7 to 9.5 eV using both a laboratory and a synchrotron ellipsometer. This procedure is preferable over near-normal incidence reflectivity measurements for materials where the reflecting surface cannot be prepared by cleavage. The reflectivity of two different UGa_3 samples with different surface preparation has been calculated from the measured complex optical conductivity. A dependence of the reflectivity on the surface preparation has been observed.

The measured components of the complex optical conductivity are compared to a calculation of the spectra from first-principles band-structure theory. The measured σ_1 and σ_2 decrease stronger at higher energies than the first-principles spectra. While we have done our best to prepare the reflecting surface as well as possible, we anticipate that this decrease is related to the still not perfect surface. The energy positions of the three typifying peaks in the measured σ_1, however, should not depend on this. These three peaks are predicted by our *ab initio* calculation. The overall good agreement between measured and calculated spectra leads us to conclude that the $5f$ electrons in UGa_3 are itinerant. Our conclusion concerning the nature of the $5f$ electrons in UGa_3—and the magnetism induced by them—is consistent with a number of other experiments which all suggest itineracy.[1,5,6,8,12] UGa_3 is therefore a prominent example of a uranium intermetallic compound having itinerant $5f$ electrons. This is an unusual finding, especially in view of the large lattice constant $a_0 = 4.248$ Å and the large U-U distance. In the calculated band structure the $5f$'s form a narrow band at the Fermi energy that is hybridized with the Ga valence bands.[11,12] From the rather good agreement between measured and calculated optical spectra we also conclude that the hybridization of the $5f$'s with the gallide spd orbitals is indeed responsible for the delocalization, as predicted by band-structure theory. Such a delocalization mechanism was previously already proposed for the UGe_3 and URh_3 compounds.[33,34]

ACKNOWLEDGMENTS

The authors thank the group of Cardona, Johnson, Richter, and Jungk for the use of their ellipsometer at BESSY and T. Wethkamp, K. Wilmers, and N. Esser for their advice. We are indebted to R. Schulz for the polishing of the sample and to BESSY GmbH for beam time and financial support. This work was sponsored by the Polish State Committee for Scientific Research under Grant No. 2P03B 150 17.

[1] A. Murasik, J. Leciejewicz, S. Ligenza, and A. Zygmunt, Phys. Status Solidi A **23**, K147 (1974).

[2] P. Dervenegas, D. Kaczorowski, F. Bourdarot, P. Burlet, A. Czopnik, and G. H. Lander, Physica B **269**, 368 (1999).

[3] K. H. J. Buschow and H. J. van Daal, in *Magnetism and Magnetic Materials*, edited by D. C. Graham and J. J. Rhyne, AIP Conf. Proc. No. 5 (AIP, New York, 1972), p. 1464.

[4] H. R. Ott, F. Hulliger, H. Rudigier, and Z. Fisk, Phys. Rev. B **31**, 1329 (1985).

[5] D. Kaczorowski, R. Troć, D. Badurski, A. Böhm, L. Shlyk, and F. Steglich, Phys. Rev. B **48**, 16 425 (1993).

[6] D. Kaczorowski, R. Hauser, and A. Czopnik, Physica B **230-232**, 35 (1997).

[7] D. Kaczorowski, P. W. Klamut, A. Czopnik, and A. Jeżowski, J. Magn. Magn. Mater. **177-181**, 41 (1998).

[8] S. Coad, A. Hiess, P. J. Brown, F. Bourdarot, P. Burlet, G. H.

Lander, M. S. S. Brooks, D. Kaczorowski, A. Czopnik, and R. Troć (unpublished).
[9] M. Divis, Phys. Status Solidi B **182**, K15 (1994).
[10] G. E. Grechnev, A. S. Panfilov, I. V. Svechkarev, D. Kaczorowski, R. Troć, and A. Czopnik, J. Magn. Magn. Mater. **157/158**, 702 (1996).
[11] G. E. Grechnev, A. S. Panfilov, I. V. Svechkarev, A. Delin, B. Johansson, J. M. Wills, and O. Eriksson, J. Magn. Magn. Mater. **192**, 137 (1999).
[12] A. L. Cornelius, A. J. Arko, J. L. Sarrao, J. D. Thompson, M. F. Hundley, C. H. Booth, N. Harrison, and P. M. Oppeneer, Phys. Rev. B **59**, 14 473 (1999).
[13] J. Schoenes, in *Handbook on the Physics and Chemistry of the Actinides*, edited by A. J. Freeman and G. H. Lander (North-Holland, Amsterdam, 1984), Vol. 1, p. 341.
[14] M. Vergöhl and J. Schoenes, J. Magn. Soc. Jpn. **20**, S1, 141 (1996).
[15] P. Beckmann and A. Spizzichino, *The Scattering of Electromagnetic Waves from Rough Surfaces* (Artech House, Norwood, MA, 1987).
[16] M. Born, *Optik* (Springer-Verlag, Berlin, 1965).
[17] J. Schoenes and F. J. Schoenes, Optik (Stuttgart) **36**, 268 (1972).
[18] R. L. Johnson, J. Barth, M. Cardona, D. Fuchs, and A. M. Bradshaw, Rev. Sci. Instrum. **60**, 2209 (1989).
[19] W. Kohn and L. Sham, Phys. Rev. **140**, A1133 (1965).
[20] U. von Barth and L. A. Hedin, J. Phys. C **5**, 1692 (1972).
[21] B. R. Cooper, Q. G. Sheng, S. P. Lim, C. Sanchez-Castro, N. Kioussis, and J. M. Wills, J. Magn. Magn. Mater. **108**, 10 (1992).
[22] M. S. S. Brooks, T. Gasche, and B. Johansson, J. Phys. Chem. Solids **56**, 1491 (1995).
[23] T. Kraft, P. M. Oppeneer, V. N. Antonov, and H. Eschrig, Phys. Rev. B **52**, 3561 (1995).
[24] P. M. Oppeneer, V. N. Antonov, A. Y. Perlov, A. N. Yaresko, T. Kraft, and H. Eschrig, Physica B **230-232**, 544 (1997).
[25] A. Delin, P. M. Oppeneer, M. S. S. Brooks, T. Kraft, B. Johansson, and O. Eriksson, Phys. Rev. B **55**, R10 173 (1997).
[26] P. M. Oppeneer, A. Y. Perlov, V. N. Antonov, A. N. Yaresko, T. Kraft, and M. S. S. Brooks, J. Alloys Compd. **271-273**, 831 (1998).
[27] P. M. Oppeneer, M S. S. Brooks, V. N. Antonov, T. Kraft, and H. Eschrig, Phys. Rev. B **53**, R10 437 (1996).
[28] J. Köhler, L. M. Sandratskii, and J. Kübler, Phys. Rev. B **55**, R10 153 (1997).
[29] P. M. Oppeneer, T. Maurer, J. Sticht, and J. Kübler, Phys. Rev. B **45**, 10 924 (1992).
[30] A. R. Williams, J. Kübler, and C. D. Gelatt, Phys. Rev. B **19**, 6094 (1979).
[31] J. Schoenes, Phys. Rep. **66**, 187 (1980).
[32] Å. Fåldt and P. O. Nilson, J. Phys. F: Met. Phys. **10**, 2573 (1980).
[33] D. D. Koelling, B. D. Dunlap, and G. W. Crabtree, Phys. Rev. B **31**, 4966 (1985).
[34] A. J. Arko, D. D. Koelling, and J. E. Schirber, in *Handbook on the Physics and Chemistry of the Actinides*, edited by A. J. Freeman and G. H. Lander (North-Holland, Amsterdam, 1985), Vol. 2, Chap. 3, p. 175.